

Interference effects in the resonant-tunneling spectrum

Jih-Chen Chiang

Department of Physics, National Sun Yat-sen University, Kaohsiung, Taiwan, Republic of China

Yia-Chung Chang

*Department of Physics and Materials Research Laboratory, University of Illinois at Urbana-Champaign,
1110 West Green Street, Urbana, Illinois 61801*

(Received 8 September 1992)

We have developed a two-band effective-mass model to study the resonant-tunneling spectra for a structure in which the interaction of a heavy-mass state (nearly discrete) with a light-mass continuum leads to interesting interference effects. We found two types of interference effects: Type I exhibits a zero-transmission dip preceding a resonance-tunneling peak and type-II exhibits a zero-transmission dip following a resonance-tunneling peak. Our theory demonstrates that by analyzing the interference structure in the resonant-tunneling spectra one can obtain a direct measurement of the strength of band mixing in semiconductor heterostructures.

I. INTRODUCTION

The resonant-tunneling spectrum shows interesting interference effects when two bands of electronic states associated with substantially different effective masses interact with each other. This phenomenon is readily seen in the InAs-GaSb-InAs tunnel structures in which a light-hole (LH) band interacts with a heavy-hole (HH) band.¹ For example, Fig. 8 of Ref. 1 shows that the LH1 resonance spectrum (solid lines) is chopped into two parts at $k_{\parallel} = (0.0075, 0)2\pi/a$ due to the mixing of HH2 and LH1 states. Recently, we have also found some very interesting interference behaviors in the transmission coefficient spectrum in Si-Ge-Si(001) strained double-barrier tunnel structures.² We found a "dip" structure followed by a double-peak structure as a result of an intervalley mixing effect. The above features can all be interpreted as an interference effect similar to the Fano resonance effect³ seen in absorption spectra when a discrete state interacts with a continuum. In this paper we use a two-band effective-mass model^{4,5} to analyze the resonant-tunneling effect for a heavy-mass (HM) band weakly coupled to a light-mass (LM) band.

II. TWO-BAND EFFECTIVE-MASS MODEL

We divide the resonant-tunneling structures into three regions: a semi-infinite region on the left, a semi-infinite region on the right, and a central region. We assume there are only two states (LM and HM) denoted by $|1; q\rangle$ and $|2; q\rangle$ associated with each q (the component of wave vector along the growth direction), where $q = K(K')$ in the left and right regions and $q = k(k')$ in the central region.

In the central region, the effective masses of LM and HM bands are labeled by m_l and m_h , respectively. If we introduce an interaction between $|1; k\rangle$ and $|2; k\rangle$, these two states will be mixed, and tunneling will happen via

these new mixed states. The new mixed state with energy E and wave vector k is denoted $|E; k\rangle$, which is the linear combination of $|1; k\rangle$ and $|2; k\rangle$ ($|E; k\rangle = c|1; k\rangle + d|2; k\rangle$). We shall denote the minimum (or maximum) of the LM band as V_0 and that of the HM band as E_0 . If the interaction H' is given, the Schrödinger equation can be written as

$$\begin{bmatrix} (k^2/2\mu_l) + V_0 & H' \\ H'^{\dagger} & (k^2/2\mu_h) + E_0 \end{bmatrix} \begin{bmatrix} c \\ d \end{bmatrix} = E \begin{bmatrix} c \\ d \end{bmatrix}, \quad (1)$$

where $\mu_l = m_l/\hbar^2$ and $\mu_h = m_h/\hbar^2$.

In this paper, we have done the calculations for the cases $H' = \beta$ and $H' = i\alpha k$, where α and β are coupling constants. The dispersion relations of E and k can be easily derived from the equation above:

$$\frac{k^4}{4\mu_l\mu_h} + \left[\frac{E'_0 - E'}{2\mu_l} - \frac{E'}{2\mu_h} \right] k^2 + E'(E' - E'_0) - \beta^2 = 0, \quad H' = \beta, \quad (2)$$

$$\frac{k^4}{4\mu_l\mu_h} + \left[\frac{E'_0 - E'}{2\mu_l} - \frac{E'}{2\mu_h} - \alpha^2 \right] k^2 + E'(E' - E'_0) = 0, \quad H' = i\alpha k, \quad (3)$$

where $E' = E - V_0$ and $E'_0 = E_0 - V_0$.

III. TRANSMISSION COEFFICIENT

In the central region, for a given energy E we can always find two mixed states associated with two wave vectors k and k' . k and k' are complex numbers in general. From now on we shall denote these two mixed states by $|E; k\rangle = c|1; k\rangle + d|2; k\rangle$ and $|E; k'\rangle = c'|1; k'\rangle + d'|2; k'\rangle$; the coefficients c , d , c' , and d' can be found by substituting (2) or (3) into (1).

For simplicity, we assume that there is no coupling between LM and HM bands in the left and right regions

and we only consider an incident electron (or hole) via a LM state. We denote the effective masses of LM and HM bands in the left and right regions as M and M' and their band minima (maximum) as U and U' , respectively. For a given energy E (for an incident electron or hole) the two possible wave vectors are $K = \sqrt{2\mu(E-U)}$ and $K' = \sqrt{2\mu'(E-U')}$, where $\mu = M/\hbar^2$ and $\mu' = M'/\hbar^2$. The wave functions $\Psi(E)$ and $\underline{J}\Psi(E)$ must be continuous across the interfaces, where the current density operator

\underline{J} can be written as⁶

$$\underline{J} = \frac{1}{\hbar} \begin{bmatrix} k/\mu_l & i\alpha \\ -i\alpha & k/\mu_h \end{bmatrix} \text{ for } H' = i\alpha k + \beta. \quad (4)$$

If a particle incidents from the left, the transmission coefficient (T) equations can be derived for both (a) $H' = \beta$ and (b) $H' = i\alpha k$.

(a) $H' = \beta$:

$$T = \frac{|(cd' - dc')(cd'S_{22} - dc'S_{21})|^2}{|(cd'S_{11} - c'dS_{12})(cd'S_{22} - c'dS_{21}) - cc'dd'(S'_{11} - S'_{12})(S'_{22} - S'_{21})|^2}, \quad (5)$$

where

$$\begin{aligned} S_{11} &= \cos(kL) - i(\bar{K}/k + k/\bar{K})\sin(kL)/2, \\ S_{12} &= \cos(k'L) - i(\bar{K}/k' + k'/\bar{K})\sin(k'L)/2, \\ S_{21} &= \cos(kL) - i(\bar{K}'/k + k/\bar{K}')\sin(kL)/2, \\ S_{22} &= \cos(k'L) - i(\bar{K}'/k' + k'/\bar{K}')\sin(k'L)/2, \\ S'_{11} &= (1 + \bar{K}'/\bar{K})\cos(kL)/2 - i(\bar{K}'/k + k/\bar{K})\sin(kL)/2, \\ S'_{12} &= (1 + \bar{K}'/\bar{K})\cos(k'L)/2 - i(\bar{K}'/k' + k'/\bar{K})\sin(k'L)/2, \\ S'_{21} &= (1 + \bar{K}/\bar{K}')\cos(kL)/2 - i(\bar{K}/k + k/\bar{K}')\sin(kL)/2, \\ S'_{22} &= (1 + \bar{K}/\bar{K}')\cos(k'L)/2 - i(\bar{K}/k' + k'/\bar{K}')\sin(k'L)/2. \end{aligned}$$

In the above equations we have defined $\bar{K} = K\mu_l/\mu$ and $\bar{K}' = K'\mu_h/\mu'$.

(b) $H' = i\alpha k$:

$$T = \frac{|(cd'S_{22} - dc'S_{21})|^2}{|(cd'S_{11} - c'dS_{12})(cd'S_{22} - c'dS_{21}) - cc'dd'(S'_{11} - S'_{12})(S'_{22} - S'_{21})|^2}, \quad (6)$$

where

$$\begin{aligned} S_{11} &= (q_2'/Y + q_1/X)\cos(kL)/2 \\ &\quad - i(\bar{K}/X + q_1q_2'/\bar{K}Y)\sin(kL)/2, \\ S_{12} &= (q_2/Y + q_1'/X)\cos(k'L)/2 \\ &\quad - i(\bar{K}'/X + q_1'q_2/\bar{K}'Y)\sin(k'L)/2, \\ S_{21} &= (q_2/Y + q_1'/X)\cos(kL)/2 \\ &\quad - i(\bar{K}'/Y + q_1'q_2/\bar{K}'X)\sin(kL)/2, \\ S_{22} &= (q_1/X + q_2'/Y)\cos(k'L)/2 \\ &\quad - i(\bar{K}/Y + q_1q_2'/\bar{K}X)\sin(k'L)/2, \\ S'_{11} &= (\bar{K}'/Y + q_1q_1'/\bar{K}'X)\cos(kL)/2 \\ &\quad - i(q_1'/X + \bar{K}'q_1/\bar{K}'Y)\sin(kL)/2, \\ S'_{12} &= (\bar{K}'/Y + q_1q_1'/\bar{K}'X)\cos(k'L)/2 \\ &\quad - i(q_1/X + \bar{K}'q_1'/\bar{K}'Y)\sin(k'L)/2, \\ S'_{21} &= (\bar{K}/X + q_2q_2'/\bar{K}Y)\cos(kL)/2 \\ &\quad - i(q_2'/Y + \bar{K}q_2/\bar{K}X)\sin(kL)/2, \end{aligned}$$

$$\begin{aligned} S'_{22} &= (\bar{K}/X + q_2q_2'/\bar{K}Y)\cos(k'L)/2 \\ &\quad - i(q_2/Y + \bar{K}q_2'/\bar{K}X)\sin(k'L)/2. \end{aligned}$$

In the above equations we have defined $\bar{K} = K\mu_l/\mu$, $\bar{K}' = K'\mu_h/\mu'$, $q_1 = k + i\alpha\mu_l d/c$, $q_1' = k' + i\alpha\mu_l d'/c'$, $q_2 = k - i\alpha\mu_h c/d$, $q_2' = k' - i\alpha\mu_h c'/d'$, $Y = cd'q_2' - dc'q_2$, and $X = cd'q_1 - c'dq_1'$.

We now apply our theory to the following two systems: (i) the $\text{Ga}_{0.52}\text{In}_{0.48}\text{As}-\text{Ga}_{0.37}\text{In}_{0.63}\text{As}_{0.87}\text{P}_{0.13}-\text{Ga}_{0.52}\text{In}_{0.48}\text{As}$ strained-layer tunnel structure (grown on InP) and (ii) the broken-gap $\text{InAs}-\text{GaSb}-\text{InAs}$ tunnel structures. Schematic diagrams of the effective potentials for the electron or hole for the above structures are shown in Fig. 1. We define k_z as the projection of the wave vector \mathbf{k} in the growth direction, k_x and k_y as two in-plane components of the wave vector, and $k_{\parallel} = (k_x^2 + k_y^2)^{1/2}$.

(i) $\text{Ga}_{0.52}\text{In}_{0.48}\text{As}-\text{Ga}_{0.37}\text{In}_{0.63}\text{As}_{0.87}\text{P}_{0.13}-\text{Ga}_{0.52}\text{In}_{0.48}\text{As}$ grown on InP. Consider a $\text{Ga}_x\text{In}_{1-x}\text{As}_y\text{P}_{1-y}$ strained layer [for which the lattice constant is $a(x,y)$] grown on InP (with lattice constant a_0) along the [001] direction; we define

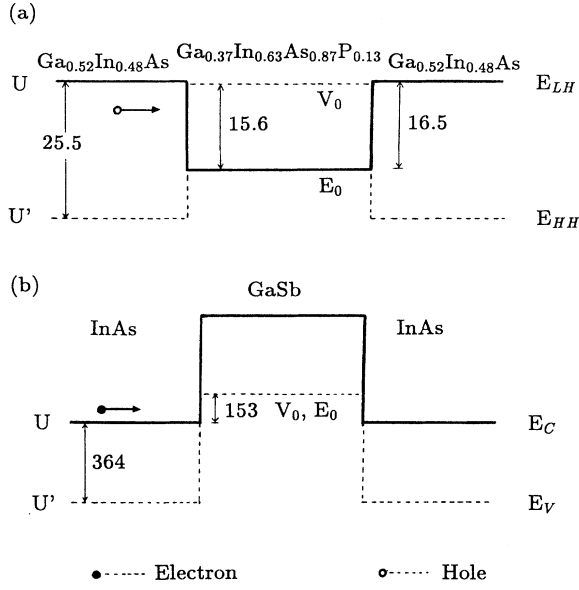


FIG. 1. Schematic energy diagram for (a) $\text{Ga}_{0.52}\text{In}_{0.48}\text{As}-\text{Ga}_{0.37}\text{In}_{0.63}\text{As}_{0.87}\text{P}_{0.13}-\text{Ga}_{0.52}\text{In}_{0.48}\text{As}$, and (b) $\text{InAs}-\text{GaSb}-\text{InAs}$ tunnel structures. The energy separations as indicated are in meV.

$$\delta E_{\text{hy}} = -2a \left[\frac{1-C_{12}}{C_{11}} \right] \left[\frac{a_0 - a(x,y)}{a_0} \right], \quad (7)$$

$$\delta E_{\text{sh}} = -2b \left[\frac{1+2C_{12}}{C_{11}} \right] \left[\frac{a_0 - a(x,y)}{a_0} \right], \quad (8)$$

where C_{11} and C_{12} are elastic stiffness components, and a and b are hydrostatic and shear deformation potentials, respectively. The coupled Schrödinger equation for HH and LH states for $\text{Ga}_x\text{In}_{1-x}\text{As}_y\text{P}_{1-y}$ (in the central region) can be written as⁶

$$- \begin{bmatrix} P - Q - \frac{\delta E_{\text{hy}}}{3} - \frac{\delta E_{\text{sh}}}{2} & \tilde{R} \\ \tilde{R}^\dagger & P + Q - \frac{\delta E_{\text{hy}}}{3} + \frac{\delta E_{\text{sh}}}{2} \end{bmatrix} \begin{bmatrix} c \\ d \end{bmatrix} = (E - V) \begin{bmatrix} c \\ d \end{bmatrix}, \quad (9)$$

where $P = \gamma_1 \hbar^2 k^2 / 2m_0$, $Q = \gamma_2 \hbar^2 (k_x^2 + k_y^2 - 2k_z^2) / 2m_0$, $\tilde{R} = \sqrt{3} \hbar^2 (\bar{\gamma} k_{\parallel}^2 - 2i\gamma_3 k_{\parallel} k_z) / 2m_0$. m_0 is the free-electron mass, γ_1 , γ_2 , and γ_3 are the Luttinger parameters, and $\bar{\gamma} = (\gamma_1 + \gamma_2) / 2$. An axial approximation⁷ has been made in the above equation.

For the $\text{Ga}_{0.52}\text{In}_{0.48}\text{As}-\text{Ga}_{0.37}\text{In}_{0.63}\text{As}_{0.87}\text{P}_{0.13}-\text{Ga}_{0.52}\text{In}_{0.48}\text{As}$ strained-layer tunnel structure, if we choose the $\text{Ga}_{0.52}\text{In}_{0.48}\text{As}$ LH band maximum as the energy zero, we can obtain the following relations by comparing (1) with (9):

$$V_0 = V + \left[\frac{\delta E_{\text{hy}}}{3} + \frac{\delta E_{\text{sh}}}{2} - \frac{(\gamma_1 - \gamma_2) \hbar^2 k_{\parallel}^2}{2m_0} \right]_{x=0.37, y=0.87}, \quad (10)$$

$$E_0 = V + \left[\frac{\delta E_{\text{hy}}}{3} - \frac{\delta E_{\text{sh}}}{2} - \frac{(\gamma_1 + \gamma_2) \hbar^2 k_{\parallel}^2}{2m_0} \right]_{x=0.37, y=0.87}, \quad (11)$$

$$m_l = \left[\frac{-m_0}{\gamma_1 + 2\gamma_2} \right]_{x=0.37, y=0.87}, \quad (12)$$

$$m_h = \left[\frac{-m_0}{\gamma_1 - 2\gamma_2} \right]_{x=0.37, y=0.87}, \quad (13)$$

$$\alpha \approx \left[\frac{\sqrt{3}\gamma_3 \hbar^2 k_{\parallel}}{m_0} \right]_{x=0.37, y=0.87}, \quad (14)$$

$$\beta \approx \left[\frac{\sqrt{3}\bar{\gamma} \hbar^2 k_{\parallel}}{2m_0} \right]_{x=0.37, y=0.87}, \quad (15)$$

where $V = 0.64\Delta E_g - [(\delta E_{\text{hy}}/3) + (\delta E_{\text{sh}}/2)]_{x=0.52, y=1}$ and ΔE_g is the band-gap discontinuity between $\text{Ga}_{0.52}\text{In}_{0.48}\text{As}$ and $\text{Ga}_{0.37}\text{In}_{0.63}\text{As}_{0.87}\text{P}_{0.13}$. Similarly in the left and right regions ($\text{Ga}_{0.52}\text{In}_{0.48}\text{As}$) we can obtain the following relations:

$$U \approx \left[-\frac{(\gamma_1 - \gamma_2) \hbar^2 k_{\parallel}^2}{2m_0} \right]_{x=0.52, y=1}, \quad (16)$$

$$U' \approx \left[-\delta E_{\text{sh}} - \frac{(\gamma_1 + \gamma_2) \hbar^2 k_{\parallel}^2}{2m_0} \right]_{x=0.52, y=1}, \quad (17)$$

$$M = \left[\frac{-m_0}{\gamma_1 + 2\gamma_2} \right]_{x=0.52, y=1}, \quad (18)$$

$$M' = \left[\frac{-m_0}{\gamma_1 - 2\gamma_2} \right]_{x=0.52, y=1}. \quad (19)$$

Note that in this tunnel structure, all the quaternary material parameters (Q) are derived from the four binary parameters (B) by using the interpolation scheme⁸

$$Q(x,y) = xyB_{AC} + x(1-y)B_{AD} + (1-x)yB_{BC} + (1-x)(1-y)B_{BD} \quad (20)$$

for a quaternary material $A_x B_{1-x} C_y D_{1-y}$. Table I shows binary parameters used here which are mainly taken from Ref. 9.

We would also like to point out that the quaternary parameters have been chosen to make $E_0 \approx U = 0$ for $k_{\parallel} = 0$. Since the HH band is below the LH band ($U' < U$) in the left and right regions due to the tensile strain and the LH band is below the HH band ($V_0 < E_0$) in the central region due to the compression strain, this tunnel structure is actually a quantum well for the HH band but a single barrier for the LH band. For small k_{\parallel} , this is a good structure to study the tunneling interference effect for which a HM state (nearly discrete) is weakly coupled to a LM continuum.

TABLE I. Parameters of InAs, GaAs, InP, and GaP.

| Parameters | InAs | GaAs | InP | GaP |
|--|--------|--------|--------|--------|
| a_0 (Å) | 6.0584 | 5.6533 | 5.8688 | 5.4512 |
| a (eV) | -6.0 | -9.77 | -9.3 | -6.35 |
| b (eV) | -1.8 | -1.7 | -2.0 | -1.5 |
| E_g (eV) | 0.36 | 1.42 | 1.35 | 2.74 |
| γ_1 | 20.4 | 6.85 | 4.95 | 4.05 |
| γ_2 | 8.3 | 2.1 | 1.65 | 0.4 |
| γ_3 | 9.1 | 2.9 | 2.35 | 1.25 |
| C_{11} (10^{11} dyn/cm ²) | 8.329 | 11.88 | 10.22 | 14.12 |
| C_{12} (10^{11} dyn/cm ²) | 4.526 | 5.38 | 5.76 | 6.253 |

(ii) *InAs-GaSb-InAs*. For convenience we choose the InAs conduction-band minimum as the energy zero, and the GaSb valence-band maximum is $V=0.154$ eV. If we assume there is weak coupling between HH and LH states for GaSb (the central region), then (1) can also be written as^{6,7,10-13}

$$-\begin{bmatrix} P-Q & \tilde{R} \\ \tilde{R}^\dagger & P+Q \end{bmatrix} \begin{bmatrix} c \\ d \end{bmatrix} = (E-V) \begin{bmatrix} c \\ d \end{bmatrix}. \quad (21)$$

For small k_{\parallel} , we obtain the following relations by comparing (1) with (20):

$$m_l = -m_0/(\gamma_1 + 2\gamma_2), \quad (22)$$

$$m_h = -m_0/(\gamma_1 - 2\gamma_2), \quad (23)$$

$$V_0 = V - (\gamma_1 - \gamma_2)\hbar^2 k_{\parallel}^2 / m_0, \quad (24)$$

$$E_0 = V - (\gamma_1 + \gamma_2)\hbar^2 k_{\parallel}^2 / m_0, \quad (25)$$

$$\alpha \approx \sqrt{3}\gamma_3\hbar^2 k_{\parallel} / m_0. \quad (26)$$

In the InAs region, we use $M=0.023m_0$, $M'=-0.36m_0$, $U' \approx -360$ meV = negative energy gap of InAs, and $U \approx \hbar^2 k_{\parallel}^2 / 2M$.

In the InAs-GaSb-InAs tunnel structure an electron in the InAs conduction band, incident from the left, tunnels through GaSb via the GaSb LH band and then returns to the InAs conduction band to the right. The tunneling process is possible because of the coupling between the conduction and LH bands at finite wave vectors (see Ref. 14). If we ignore the weak coupling between the conduction and HH bands for small k_{\parallel} , the wave function of an InAs bulk state consists of both conduction and LH components, and the Schrödinger equation in a $\mathbf{k}\cdot\mathbf{p}$ theory can be written as^{4,14}

$$\begin{bmatrix} E_c - E & it\hbar q \\ -it\hbar q & E_v - E \end{bmatrix} \begin{bmatrix} \Psi_c \\ \Psi_v \end{bmatrix} = 0, \quad (27)$$

where Ψ_c and Ψ_v are the conduction-band and light-hole-band components of the total wave function, and E_c and E_v are the conduction-band minimum and light-hole-band maximum, respectively. The parameter t reflects the strength of the coupling between the conduction and LH bands. In Bastard's model, the same value of t is used for all constituent materials.⁴ To ensure the continuity of current density and light-hole-band com-

ponent of the total wave function across the interfaces, the sufficient condition is that $2(E-E_v)\Psi_v/\hbar q$ and $\Psi_v(E)$ are continuous across the interfaces. Note that the continuity of Ψ_c is automatically satisfied since a single value of t has been used for both InAs and GaSb. Since the incident electron energy E is very close to the GaSb LH band maximum, E_v in the central region, $(E-E_v) \approx \hbar^2 k^2 / 2m_l$, and $2(E-E_v)(\Psi_v/\hbar k) \approx \hbar k \Psi_v / m_l$. But the incident electron energy E is far from the InAs LH band maximum, E_v in the left or right region; the boundary condition used in the derivations of (5) and (6) must be modified, and we need to replace $\tilde{K} = K\mu_l/\mu$ by $\tilde{K} = 2\mu(E-U')/K$.

IV. RESULTS AND DISCUSSIONS

(a) $H' = \beta$. Figure 2 shows the transmission coefficient as a function of hole energy for hole tunneling through valence bands of a $\text{Ga}_{0.52}\text{In}_{0.48}\text{As}-\text{Ga}_{0.37}\text{In}_{0.63}\text{As}_{0.87}\text{P}_{0.13}-\text{Ga}_{0.52}\text{In}_{0.48}\text{As}$ tunnel structure (grown on InP), in which a weak coupling (with $\beta=3$ meV) between the HM and LM states exists in the central region. Here we have ignored the iak term in H_1 , which is valid when $k_{\parallel} \gg k_z$. A weak-coupling limit is defined when $\beta \ll \Delta E$, where ΔE is the energy separation between the two consecutive quantum confined levels in the central region. The following material parameters have been used: $m_l = -0.041m_0$, $m_h = -0.31m_0$, $M = -0.043m_0$, $M' = -0.31m_0$, $L = 176$ Å, $V_0 = -16.5$ meV, $E_0 = -0.9$ meV, $U = 0$, $U' = -25.5$ meV. We found a "dip to zero" structure at the high-energy side of the HM1 resonance peak and another on the low-energy side of the HM2 resonance peak. Here HM n denotes the n th quantum confined levels associated with the HM band. Examining (5), we see that the transmission coefficient vanishes when $cd'S_{22} - dc'S_{21} = 0$. We denote the energies at which the total reflection occurs (i.e., $T=0$) as E_R . Also note that energies of HM quantum confined levels are given by the roots of $S_{22} = 0$ (denoted

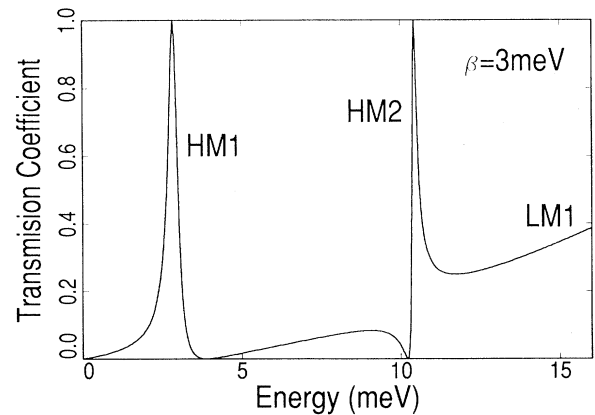


FIG. 2. Transmission coefficient as a function of hole energy for hole tunneling through valence bands of a $\text{Ga}_{0.52}\text{In}_{0.48}\text{As}-\text{Ga}_{0.37}\text{In}_{0.63}\text{As}_{0.87}\text{P}_{0.13}-\text{Ga}_{0.52}\text{In}_{0.48}\text{As}$ tunnel structure (grown on InP) with $H' = \beta = 3$ meV.

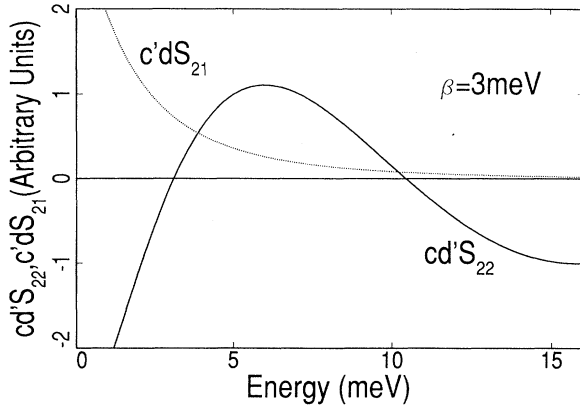


FIG. 3. $cd'S_{22}$ and $c'dS_{21}$ curves as a function of hole energy for hole tunneling through valence bands of a $\text{Ga}_{0.52}\text{In}_{0.48}\text{As-Ga}_{0.37}\text{In}_{0.63}\text{As}_{0.87}\text{P}_{0.13}\text{-Ga}_{0.52}\text{In}_{0.48}\text{As}$ tunnel structure (grown on InP) with $H'=\beta=3$ meV.

E_h) if there is no coupling between HM and LM states. Thus E_h and E_R can be determined graphically by finding the intersections of the $cd'S_{22}$ curve with the horizontal axis and with the $c'dS_{21}$ curve (see Fig. 3). Figure 3 also shows that E_R is on the high-energy side of E_h for the HM1 state and on the low-energy side of E_h for the HM2 state. These account for the positions of the dip to zero structure relative to the positions of the HM1 and HM2 resonance peaks.

Figure 4 shows the transmission coefficient for the above structure with stronger coupling constant ($\beta=7$ meV). All the other parameters are the same. In this case the dip to zero structures do not occur as a result of the stronger coupling constant β , which is comparable to the energy difference of HM2 and HM1 states. To account for this feature, we also plot the $cd'S_{22}$ and $c'dS_{21}$ curves in Fig. 5. As seen in this figure, the two curves no longer cross each other.

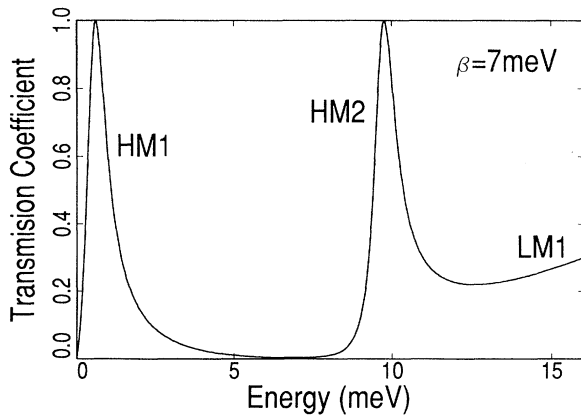


FIG. 4. Transmission coefficient as a function of hole energy for hole tunneling through valence bands of a $\text{Ga}_{0.52}\text{In}_{0.48}\text{As-Ga}_{0.37}\text{In}_{0.63}\text{As}_{0.87}\text{P}_{0.13}\text{-Ga}_{0.52}\text{In}_{0.48}\text{As}$ tunnel structure (grown on InP) with $H'=\beta=7$ meV.

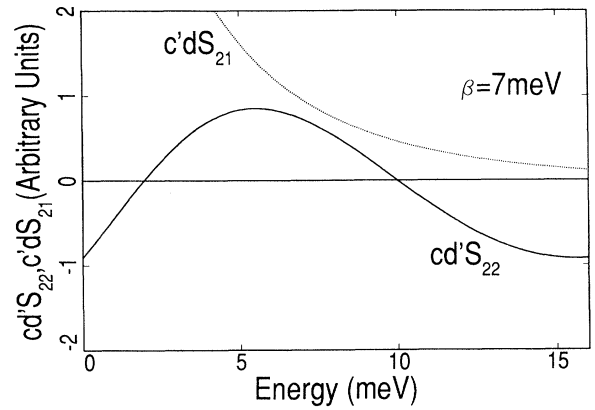


FIG. 5. $cd'S_{22}$ and $c'dS_{21}$ curves as a function of hole energy for hole tunneling through valence bands of $\text{Ga}_{0.52}\text{In}_{0.48}\text{As-Ga}_{0.37}\text{In}_{0.63}\text{As}_{0.87}\text{P}_{0.13}\text{-Ga}_{0.52}\text{In}_{0.48}\text{As}$ tunnel structure (grown on InP) with $H'=\beta=7$ meV.

(b) $H'=iak$. Figure 6 shows the transmission coefficient as a function of hole energy for hole tunneling through valence bands of $\text{Ga}_{0.52}\text{In}_{0.48}\text{As-Ga}_{0.37}\text{In}_{0.63}\text{As}_{0.87}\text{P}_{0.13}\text{-Ga}_{0.52}\text{In}_{0.48}\text{As}$ (grown on InP) strained-layer structure, in which a weak coupling (with $\alpha=0.26$ eV \AA) between the HM and LM states exists in the central region. Here we have ignored the β term in H_1 , which is valid when $k_{\parallel} \ll k_z$. The following material parameters have been used: $V_0=-16.5$ meV, $E_0=-0.9$ meV, $m_l=-0.041m_0$, $m_h=-0.31m_0$, $M=-0.043m_0$, $M'=-0.31m_0$, $L=176$ \AA , $U=-0.33$ meV, $U'=-25.5$ meV. The parameters $V_0, E_0, m_l, m_h, \alpha, U, U', M, M'$ used were obtained by using (10)–(18) with $k_x=0.006\pi/a_0, k_y=0$. The quaternary material parameters used in (10)–(18) are derived from (19) by using the binary parameters listed in Table I. We found a dip to zero structure at the low-energy side of the HM1 resonance peak and another on

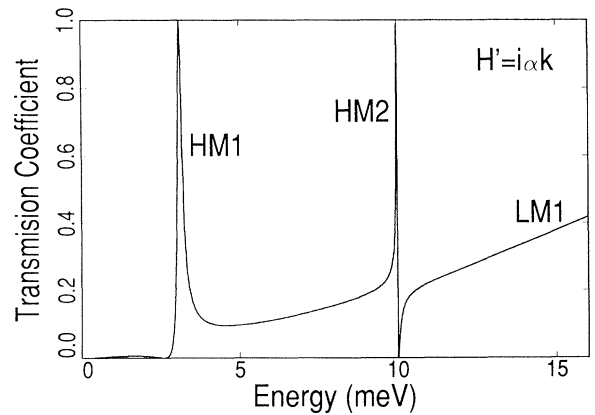


FIG. 6. Transmission coefficient as a function of hole energy for hole tunneling through valence bands of a $\text{Ga}_{0.52}\text{In}_{0.48}\text{As-Ga}_{0.37}\text{In}_{0.63}\text{As}_{0.87}\text{P}_{0.13}\text{-Ga}_{0.52}\text{In}_{0.48}\text{As}$ tunnel structure (grown on InP) with $\alpha=0.26$ eV \AA .

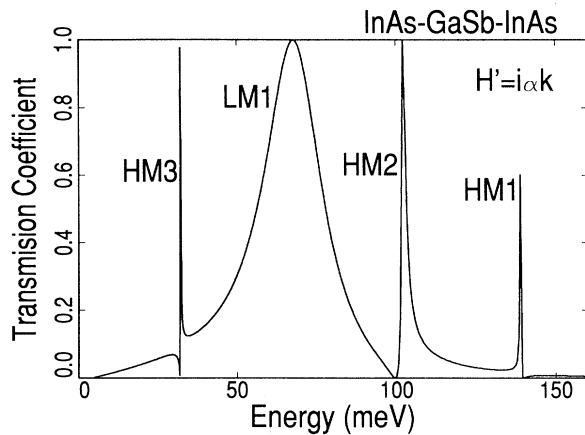


FIG. 7. Transmission coefficient for electron tunneling through valence bands of an InAs-GaSb-InAs broken-gap tunnel structure at $k_x = 0.01\pi/a$ and $k_y = 0$.

the high-energy side of the HM2 resonance peak.

Figure 7 shows the transmission coefficient for electron tunneling through valence bands of an InAs-GaSb-InAs tunnel structure, in which weak coupling (with $\alpha = 0.36$ eV Å) between the HM and LM states exists in the central region. The material parameters are as follows: $m_l = -0.055m_0$, $m_h = -0.25m_0$, $V_0 = 153$ meV, $E_0 = 152$ meV, $L = 92$ Å, $U' = -360$ meV, $U = 4.3$ meV, $M = 0.023m_0$, and $M' = -0.36m_0$. The parameters m_l , m_h , V_0 , E_0 , and α used were obtained by using (21)–(25) with $\gamma_1 = 11.1$, $\gamma_2 = 3.6$, $\gamma_3 = 5.26$, $k_x = 0.01\pi/a$, and

$k_y = 0$. The main features in Fig. 7 are the appearance of zero transmission on the high-energy side of the HM1 resonance peak and that on the low-energy side of the HM2 and HM3 resonance peaks. Similar results have been obtained by using an eight-band band-orbital model (see solid curves in Fig. 4 of Ref. 2). Here we have used $\tilde{K} = 2\mu_l(E - U')/K$ instead of $\tilde{K} - K\mu_l/\mu$ to take into account the new boundary condition. Our overall transmission coefficient spectrum is also in good agreement with that obtained by the more complicated eight-band model.

V. SUMMARY

Our main conclusion is that the interference effects due to the coupling of a HM state with a LM state in the central region of a tunnel structure can lead to a “dip to zero” structure on either side of the HM resonance peak in the transmission coefficient spectrum. Analytic expressions for the transmission coefficients were obtained for two kinds of couplings, and the physical origin of the interference effects is illustrated. We also show that a simple two-band effective-mass model can be used to obtain transmission spectra for various tunnel structures with results comparable to those obtained by more complicated models.

ACKNOWLEDGMENTS

We would like to thank S. L. Chuang for fruitful discussions. This work was supported in part by the U.S. Office of Naval Research (ONR) under Contract No. N00014-89-J-1157.

- ¹D. Z.-Y. Ting, E. T. Yu, and T. C. McGill, *Phys. Rev. B* **45**, 3583 (1992).
²J.-C. Chiang and Y. C. Chang, *Appl. Phys. Lett.* **61**, 1045 (1992).
³U. Fano, *Phys. Rev.* **124**, 1866 (1961).
⁴G. Bastard, *Phys. Rev. B* **24**, 5693 (1981); **25**, 7584 (1982).
⁵P. Lawaetz, *Phys. Rev. B* **4**, 3460 (1971).
⁶S. L. Chuang, *Phys. Rev. B* **43**, 9649 (1991).
⁷D. A. Broido and L. J. Sham, *Phys. Rev. B* **31**, 888 (1985).
⁸Sadao Adachi, *J. Appl. Phys.* **53**, 8775 (1982).
⁹*Numerical Data and Functional Relationships in Science and Technology*, edited by K.-H. Hellwege, Landolt-Börnstein,

- New series, Group III, Vol. 17a (Springer, Berlin, 1982); Group III-IV, Vol. 22a (Springer, Berlin, 1986).
¹⁰D. Ahn and S. L. Chuang, *J. Appl. Phys.* **64**, 6143 (1988).
¹¹J. M. Luttinger and W. Kohn, *Phys. Rev.* **97**, 869 (1955).
¹²D. Ahn, S. L. Chuang, and Y. C. Chang, *J. Appl. Phys.* **64**, 4056 (1988).
¹³A. Twardowski and C. Hermann, *Phys. Rev. B* **35**, 8144 (1987).
¹⁴J. R. Söderström, E. T. Yu, M. K. Jackson, Y. Rajakarunanyake, and T. C. McGill, *J. Appl. Phys.* **68**, 1372 (1990).